TITLE: DEM/CFD approach for modeling granular flow in the revolving static mixer

AUTHORS: Milada Pezo, Lato Pezo, Aca Jovanović, Biljana Lončar, Radmilo Čolović

This article is provided by author(s) and FINS Repository in accordance with publisher policies.

The correct citation is available in the FINS Repository record for this article.

NOTICE: This is the author's version of a work that was accepted for publication in *Chemical Engineering Research and Design.* Changes resulting from the publishing process, such as peer review, editing, corrections, structural formatting, and other quality control mechanisms may not be reflected in this document. Changes may have been made to this work since it was submitted for publication. A definitive version was subsequently published in *Chemical Engineering Research and Design*, Volume 109, May 2016, Pages 317–326. DOI: 10.1016/j.cherd.2016.02.003

This item is made available to you under the Creative Commons Attribution-NonCommercial-NoDerivative Works – CC BY-NC-ND 3.0 Serbia

DEM/CFD Approach for Modeling Granular Flow in the Revolving Static Mixer

Milada Pezo[1], Lato Pezo[2*], Aca Jovanović[2], Biljana Lončar[3], Radmilo Čolović[4]
[1] Laboratory for Thermal Engineering and Energy, Institute of Nuclear Sciences "Vinča", University of Belgrade, P.O. Box 522, 11001 Belgrade, Serbia
[2] Institute of General and Physical Chemistry, University of Belgrade, Studentski Trg 12-16, 11000 Belgrade, Serbia
[3] Faculty of Technology, University of Novi Sad, Bulevar Cara Lazara 1, 21000 Novi Sad, Serbia
[4] Institute of food technology Novi Sad, University of Novi Sad, Bulevar Cara Lazara 1, 21000 Novi Sad, Serbia

*Corresponding author: Lato L. Pezo, e-mail: latopezo@yahoo.co.uk, tel/fax: +381 11 3283 185

ABSTRACT

DEM/CFD (Discrete Element Method /Computational Fluid Dynamic) approach was used to develop a three dimensional model of fluid flow and mixing process of solid particles within the revolving static mixer, type Komax. Static mixers are widely used in process industry, food industry, pharmaceutical and chemical industry. Mixing process adds significant value to the final product and it can be regarded as a key process. The quality and the price of the product often depend on mixing efficiency. Both design and operation of the mixing unit itself have a strong influence on the quality produced. In this paper, DEM is used for modeling granular flow of zeolite spheres in the revolving Komax static mixer and CFD method was used for modeling fluid flow through the Eulerian multiphase model. Coupling of these two methods provides reliable analysis of particle motion and flow pattern of the working fluid. The objective of this paper is to predict the behavior of particles after several rotations of the revolving static mixer. This type of device is used for premixing action before the main mixing process, for significant reduction of mixing time and energy consumption. This type of premixing action is not investigated in detail in the open literature. The results of the numerical simulation are compared with appropriate experimental results. The special design revolving static mixer, made of transparent Plexiglas was used for this experiment. Mixing quality was examined by RSD (relative standard deviation) criterion. Application of this model provides the optimization of the number of revolutions and geometrical parameters of mixing process taking into account the quality of the mixing process.

Keywords: DEM/CFD; Revolving static mixer; Komax; Particle tracking; Mixing quality.

NOMENCLATURE

d	diameter, m
E	Young's modulus, Pa
f	force, N
$f_{c,ij}$	contact forces, N
$f_{D,i}$	viscous drag force, N
$f_{d,ij}$	viscous damping forces, N
Fp_{-f}	volumetric fluid–particle interaction force, N
$f_{p\_f,i}$	inter-particle forces between particles i and j, N

$f_{pg,i}$ pressure gradient force, N
g acceleration due to gravity, m/s^2
I moment of inertia, kgm
m_i mass of particle, kg
M_{ij} rolling friction torque, Nm
n unit vector in the normal direction of two contact spheres, dimensionless
p pressure, Pa
R radius vector (from particle center to a contact point), m
Re Reynolds number, dimensionless
t time, s
T_{ij} torques generated by the tangential forces, Nm
u fluid velocity, m/s
u` fluctuating fluid velocity, m/s
v velocity of the particle, m/s
V volume, m^3

Greek:
β empirical coefficient defined in Table 1, dimensionless
δ vector of the particle–particle or particle–wall overlap, m
ε porosity, dimensionless
ρ density, kg/m^3
μ fluid viscosity, kg/m/s
μ_r coefficient of rolling friction, m
μ_s coefficient of sliding friction, dimensionless
τ fluid viscous stress tensor, N/m^3
ω_i rotational velocities of particle i, rad/s

Indexes:
c contact
cell cell
D drag
f fluid
i particle i
p particle
p-f fluid-particle
pg pressure gradient

INTRODUCTION

Static mixers are mixing devices used in various branches of industry, such as: process industry, chemical, food and pharmaceutical industry. They are low energy consumption and efficient mixing devices which use energy from the gravitational flow to produce the desired mixing results in the process. There are several commercial types of static mixers that can be found in the industry, but the choice of optimal type of mixer is still very complex and demanding. The engineers are trying to select the optimal mixer depending on the size and the shape of mixing particles, humidity and the purity of granules or powders. The quality of the mixing process can

be improved by adding some elements welded to the outlet of the mixing tube and/or by changing the number of elements of the mixer and/or by application of the revolving static mixer. The type of static mixer, number of elements, and the velocity of the working fluid are the primary drivers for static mixer pressure drop and mixer performance, [1,2].

Static mixers are usually placed in the long vertical tubes or cylindrical shell, and its profiled geometry affects the direction of the material flow. They can be applied in a wide range of operations in the industry, including dosing, mixing, dispersing, laminar flow, heat transfer and the formation of emulsions. The mixing process is performed by the constant splitting, expansion and transport components of the material. These mixers are single pass systems, or the systems with recirculation loop (revolving static mixers). They can be used as additional mixers or premixers, or they can be used as a total replacement of conventional mixers. These mixers are used in a laminar and in a turbulent flow, in which particle clusters are subject to division, transfer, separation, acceleration, deceleration and recombination, [1].

There is a wide range of commercial static mixers on the market that satisfies the basic criteria for mixing quality, but it is necessary to optimize their characteristics depending on the material properties and the working regime of the mixer.

The summaries on the performances of static mixers and the quantitative comparison are analyzed in [1,2]. The first patent on a static mixer was described as a single element, multilayer, motionless mixer, used to mix air with a gaseous fuel, [3]. First mixer with helical elements was patented in 1949, [4]. Static mixers were first used in petrochemical industry, [5,6,7]. There are more than 30 commercial models currently available, [8]. Komax is one of the most common type of static mixers used in the industry, because of its simple manufacture and low price.

Detailed review on static mixers, concerning the mechanisms, applications and characterization methods focusing on mixing and mass transfer performance is given in [9]. Bridgwater, [10], published a review about mixing of powders and granular materials by mechanical means. The focus was on works related to mathematical modeling and numerical simulation using Discrete Element Method. The first granular dynamics simulation technique published in the open literature was the soft-sphere method originally developed by Cundall and Strack, [11]. In this model, particles are permitted to suffer minute deformations, and these small deformations are used to calculate elastic, plastic and frictional forces between particles. Newton's laws of motion are used for modelling the motion of particles. A characteristic feature of the soft-sphere models is that they are capable of handling multiple contacts which are of importance in modeling quasi-static systems. Zhu et al, [12] published a review article concerning discrete particle simulation technique. The focus of this paper is the discrete element method and associated theoretical developments. It covers three important aspects: models for the calculation of the particle–particle and particle–fluid interaction forces, coupling of discrete element method with computational fluid dynamics to describe particle–fluid flow, and the theories for linking discrete to continuum modelling. Analysis of the mixing of solid particles with a plowshare mixer via the discrete element method (DEM) was presented in [13]. The results of the simulation were compared with the Positron Emission Particle Tracking (PEPT), [14], data reported in the literature by Laurent and Cleary, [15]. Lacey index was used as a factor to find the mixing rate, [16]. The mechanistic model for a wet granulation process, combining the techniques of population balance modeling and discrete element methods to predict critical quality attributes of the granule product, such as porosity and the size distribution was presented in [17]. DEM study of the mixing of particles induced by a flat blade is presented in [18]. Coupling CFD and DEM have proven to be powerful for analyzing the behavior of the granules and fluid, which

contributes mixing, [8,19,20,21]. The effects of particle size and density on the mixing behavior have been studied by means of the discrete element method, [22,23]. The optimization of the geometry of a rotating drum mixer to enhance mixing of particles was thoroughly analyzed, [24]. Markovian models have been applied to a wide range of powder mixers: they have been applied to static mixers, [25,26,27,28,29], to fluidised-bed mixers, [30,31], to tumbler mixers, [32,33].
Lagrangian tracking techniques have been used in many studies in order to characterize the mixing performance in different systems, [34,35,36]. The review article about the computational studies of tumbler mixing, focusing on two different techniques: Particle Dynamics and Lagrangian Simulation were presented in [37].
In this paper the enhancement of the mixing quality was achieved by adding a revolving static mixer in the regime of laminar gravitational flow. This type of device is used for premixing action before the main mixing process, for significant reducing of mixing time and energy consumption. This type of premixing action is not investigated in detail in the open literature. The two main variables for a static mixer are the mixer size and the number of elements, while the number of revolutions for a revolving static premixer are the parameters that can be optimized. The revolving static mixer is particularly convenient in the case of a limited space in which the premixer must be placed.
Mathematical modeling is the most reliable and most effective way to optimize the geometry of the mixing devices and to choose the proper equipment.
The typical industrial application of the revolving static mixer is shown on Fig. 1. Screw conveyors are used to remove powder or grain material from silos, and transport it to the weighting scale and the mixer. Before the mixing process is performed, premixing action is done, using a revolving static mixer.

A detailed review and definitions of the quality of a mixture, the mixing mechanisms, the possibilities for the choice of solid mixer, the experimental assessment of homogeneity and mixing indexes are presented in [16, 38,39].
In this paper, experimental and numerical comparison between revolving static premixer, type Komax, has been performed. The fluid is treated as a continuum, while the solid phase is modeled using the Discrete Element Method (DEM). The model is solved in two stages, first the fluid velocity and pressure field are computed by using CFD (Computational Fluid Dynamics) approach, and then, using a separate study, the particle trajectories of the granular materials are computed. The quality of the mixing process is analyzed using relative standard deviation (RSD) criteria, [38]. Each experiment was repeated for 6 times, and the results of the experiments were averaged.

EXPERIMENTAL METHOD

The experimental apparatus was specially designed for this study, using transparent Plexiglass consisted of three segments, Fig. 2a. Upper segment is divided into the two compartments with a barrier and a mobile panel. Spherical painted zeolite granules (approx. 2.5 mm) are placed in both compartments, red granules in the first compartment and blue granules in the second compartment. The granules are spheres made of synthetic zeolite, type 4A, which characteristics are given in [40]. This compartment is used only for the initial separation of the granules before the premixing. The first and third compartments are used to collect the granules before and after the premixing is done. These compartments are also made of transparent Plexiglas with a height of 180 mm. The second compartment is a premixing device, with 3 segments, each with a height

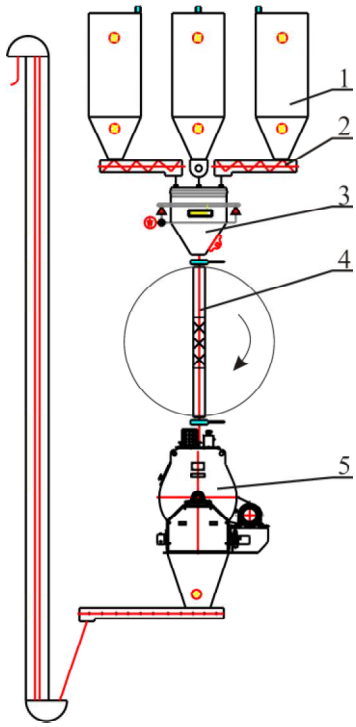

Figure 1. Schematic design of the revolving static mixer industrial application, (1) silos, (2) screw conveyor, (3) weighting scale, (4) revolving static mixer, (5) main mixer.

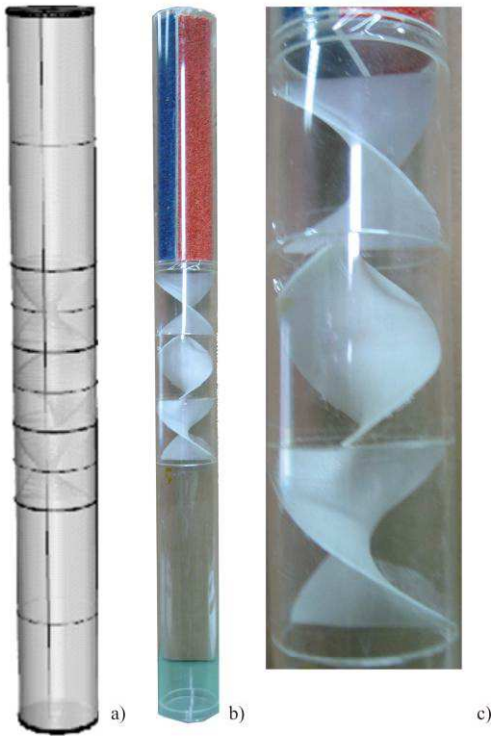

Figure 2. a) Scheme of the revolving static mixer, b) Experimental configuration, c) Komax mixer.

of 60 mm, and the outlet diameter of 60 mm. The segments are connected in the way that the outlet of the first right-handed segment is connected with second, left-handed segment, at an angle of 90 degrees relative to the vertical axis, Fig. 2b.
The revolving static premixer, type Komax, consists of three mixing elements, two right-handed Komax segments and one left-handed Komax segment. The elements are made of white plastic (ABS), in thickness of 1.5 mm, by using a 3D printing device (CubePro Trio, used for rapid prototyping). The tube in which the segments are placed is made of 3 mm transparent Plexiglas.
After passing through three segments of the static mixer, granules fall at the bottom of the lower compartment of the premixer. After that, the static mixer is rotated for 180 degrees. At that moment, the material from the upper compartment begin to pass through a static premixer under the influence of gravitational force. Rotation of the mixer is performed by hand for five times.
Fig. 2c presents the special design of the Komax static mixer used for this experiment.

DESCRIPTION OF THE MATHEMATICAL MODEL

The conditions under which the experiments were conducted correspond to the numerical simulation conditions.
Three dimensional mathematical model was used for numerical simulation. CFD approach is used for modeling gas phase. Air is treated as an ideal gas and ideal state gas equation has been applied in this model. The governing equations of gas phase are the standard Navier–Stokes equations as conservation of mass and momentum. Source term is the fluid particle interaction force defined by:

$$F_{p-f} = \frac{1}{V_{cell}} \sum_{i=1}^{k_i} \rho_{p-f,i} \tag{1}$$

where k_i is the number of particles in a CFD cell.

Contact between two particles is equivalent to the contact of two rigid bodies allowed to overlap slightly in DEM, [12]. DEM adopts simplified linear model to determine the forces and torques resulting from the contact between particles. The most common linear model is the so-called linear spring–dashpot model, [11], where the spring is used for the elastic deformation while the dashpot accounts for the viscous dissipation. Contact force can be decomposed into a component in the contact plane (or tangential plane) and one normal to the plane, thus a contact force has two components: normal and tangential. The total force and torque acting on a particle depend on many geometrical and physical parameters such as the particle shape, material properties and movement state of particles.
The solid phase is treated as a discrete phase and described by the Discrete Element Method, [11]. According to this method, the translational and rotational motions of a particle at any time, t, can be described by Newton's law of motion:

$$m_i \frac{dv_i}{dt} = f_{p-f,i} + \sum_{j=1}^{k_i} f_{c,ij} + f_{d,ij} + m_i g \tag{2}$$

and

$$I_i \frac{d\omega_i}{dt} = \sum_{j=1}^{k_i} T_{ij} + M_{ij} \tag{3}$$

where m_i, I_i, v_i and ω_i are, respectively, the mass, moment of inertia, translational and rotational velocities of particle i.

The forces acting on solids are the gas–solids interaction force, $f_{p\_f,i}$, inter-particle forces between particles i and j, include the contact forces, $f_{c,ij}$, and viscous damping forces, $f_{d,ij}$, and the gravitational force, $m_i g$. They are described in detail in the literature, [12].

Normal contact forces:

$$f_{cn,ij} = -\frac{E}{3\ 1-v^2}\sqrt{2R_i}\,\delta_n^{3/2} n \tag{4}$$

Normal viscous damping forces:

$$f_{dn,ij} = -c_n \left(\frac{3m_i E}{\sqrt{2\ 1-v^2\ \sqrt{2R\delta_n}}} \right)^{1/2} v_{n,ij} \tag{5}$$

Tangential contact forces:

$$f_{ct,ij} = -\frac{\mu_s f_{cn,ij}}{|\delta_t|}\left[1-\left(1-\frac{\min\ |\delta_t|, \delta_{t\max}}{\delta_{t,\max}} \right)^{3/2} \right]\delta_t \tag{6}$$

Tangential viscous damping forces:

$$f_{dt,ij} = -c_t \left(6m_i \mu_s f_{cn,ij} \frac{\sqrt{1-\delta_t/\delta_{t\max}}}{\delta_{t,\max}} \right)^{1/2} \cdot v_{t,ij} \tag{7}$$

$$v_{ij} = v_j - v_i + \omega_j \times R_j - \omega_i \times R_i$$

where $v_{n,ij} = v_{ij} \cdot n \cdot n$

$$v_{t,ij} = v_{ij} \times n \times n$$

In this model, the gas–solid interaction force includes the viscous drag force ($f_{D,i}$) and pressure gradient force ($f_{pg,i}$). Inter- particle forces are summed over the k_i particles in contact with particle i.

Particle–fluid interaction force:

$$f_{D,i} = \left(0.63 + \frac{4.8}{\mathrm{Re}_{p,i}^{0.5}} \right)^2 \frac{\rho_f |u_i - v_i|\ u_i - v_i}{2} \frac{\pi d_i^2}{4} \varepsilon_i^{-\beta} \tag{8}$$

$$\mathrm{Re}_{p,i} = \frac{d_i \rho_f \varepsilon_i |u_i - v_i|}{\mu_f}$$

$$\beta = 3.7 - 0.65 \exp \frac{1.5 - \log \mathrm{Re}_{p,i}}{2}^2$$

where

$$\varepsilon = 1 - \frac{\sum_{i=1}^{k_c} V_i}{\Delta V_C}$$

Pressure gradient force:

$$f_{pg,i} = V_{p,i} \nabla P \tag{9}$$

Torques, T_{ij}, are generated by the tangential forces and cause particle i to rotate because the inter-particle forces act at the contact point between particles i and j and not at the particle center. M_{ij} is the rolling friction torque that is in opposition to the rotation of i-th particle.

Torque Rolling:

$$T_{ij} = R_i \times \ f_{ct,ij} + f_{dt,ij} \tag{10}$$

Torque Friction:

$$M_{ij} = -\mu_r f_{ct,ij} \hat{\omega}_{ij} \tag{11}$$

The equations used to calculate the forces in Eqs. (2) – (11) are very much standardized now and they are listed in [41].

The fluid velocity and pressure field can be determined by standard CFD method by solving Navier–Stokes equations. A solid flow field can be obtained by solving Eqs. (2) and (3) by an explicit time integration method. The modelling of the fluid flow by CFD is at the computational cell level, whilst the modelling of the solids flow by DEM is on the individual particle level. Coupling DEM and CFD is achieved as follows: 1) DEM give information about positions, velocities and accelerations of individual particles at each time step, 2) These data are used for the evaluation of void fraction and volumetric fluid–particles interaction force in a computational cell, 3) CFD then uses these data to determine the fluid flow field which then yields the fluid forces acting on individual particles. Incorporation of the resulting forces into DEM will produce information about the motion of individual particles for the next time step, [19].

Figure 3. Rotation of the revolving static mixer.

Numerical evaluations were performed for four rotations (and five particle passes through the mixer) of the revolving static premixer. Boundary conditions are: 1) inlet -one compartment filled with 4,000 red particles and another compartment filled with 4,000 blue particles, Fig. 2b, 2)

outlet-pressure outlet (atmospheric pressure) and 3) the mixer tube and the helix of the mixer are modeled as wall (Fig. 2c). It is assumed that the helix surface is fresh aged (surface roughness affects the particle flow minimally). The gravity represents the force which leads the particles to fall into the bottom segment. The gas (air) velocity at the inlet is assumed to be zero, so that the impact of fluid flow at the beginning of the simulation of the particle movement is minimal. The gas velocity after first rotation of the mixer is determined from the data obtained at the outlet of CFD simulation.

The revolving static mixer was rotated during the experiment, according to Fig. 3.

NUMERICAL SIMULATION CONDITIONS

The set of balance equations for CFD modelling is solved by using the control volume based finite difference method. SIMPLE (Semi Implicit Method for Pressure-Linked Equations) numerical method is used for solving pressure-correction equation from the momentum and mass balance equations, [42]. The three-dimensional flow field is discretized in Cartesian coordinates. Numerical grids are made from 50,870 control volumes. Optimization of the numerical grid was performed, and grid refinement tests showed that there are no significant changes in the results of the simulation for larger number of cells in control volume. Elements used in numerical mesh are tetrahedral and the size of an element is less than 10^{-8} m^3.

A discretization of partial differential equations is carried out by their integration over control volumes of basic and staggered grids. The convection terms are approximated with upwind finite differences, while diffusion and source terms are approximated with central differences. Fully implicit time integration is applied. The set of algebraic equations is solved iteratively with the line-by-line TDMA (Three-Diagonal-Matrix Algorithm), [42].

The calculation error for every balance equation and every control volume is kept within limits of 10^{-5} by iterative solution of sets of linear algebraic equations.

The DEM require much smaller time step than CFD. CFD time step is ten times larger than the DEM time step. The DEM time step is limited by the natural oscillation period of spring-mass system used to model contacting particles. It should satisfy the following equation

$$\Delta t_{DEM} \leq \frac{1}{10} 2\pi \sqrt{\frac{m}{k}} \tag{12}$$

where m is particle mass and k is stiffness coefficient. Simulation conditions and parameters of the mixing process are given in Table 1.

These parameters of DEM simulation are written in Table 1. The zeolite particles are almost perfect spheres, with very similar diameters of all particles. The coefficients which represent the collision phenomena were investigated experimentally (elastic coefficient, damping coefficient, friction coefficient, rolling friction coefficient, restitution coefficient and angle of repose), Table 1.

In this study, the experimental determination of the restitution coefficient was performed using the method in detail explained in the research of Smith and Liu, [43]. There are also a few literature known methods that could be used for coefficients representing the inter-particle and particle to wall collision phenomena, [43-45]. The friction coefficient for particles was determined using the method explained in the work of Mohsenin, [46]. The particle to wall friction coefficient was obtained using the method explained in the work of Stahl, [47]. The

rolling friction coefficient was determined using the method described in the study of Jiang, Yu and Harris, [48]. Within the numerical simulation, it was presumed that the tangential contact parameters are equal to normal contact parameters. The humidity of the zeolite granules is also determined experimentally, and the value was written within Table 1.

Table 1.
Simulation conditions and parameters of modeling process

Parameter	Value
Size of the mixer r×l, mm×mm	60x280
Particle number	8,000
Particle diameter, mm	2.5
Particle density, kg/m^3	650
Fluid velocity, m/s	0
CFD time step, s	5×10^{-5}
DEM time step, s	5×10^{-6}
Fluid density, kg/m^3	1.2
Fluid viscosity, kg/ms	1.8×10^{-5}
Particle friction coefficient	0.3
Particle rolling friction coefficient	0.3
Particle elastic coefficient	0.3
Particle damping coefficient	0.25
Restitution coefficient	0.5
Angle of repose	22^o
Particle - wall friction coefficient	0.3
Particle - wall elastic coefficient	0.3
Particle - wall damping coefficient	0.25
Young's modulus	10^7
Poisson's ratio of particles	0.25
Humidity of zelite granules	8.5%

RESULTS AND DISCUSSIONS

Numerical simulations were performed for static mixer after one, two, three and four rotations (maximum five material passes). This type of mixer is used for pre-mixing and mixing quality depends on the number of rotations. The results of DEM/CFD modeling were compared with experimental results. The photographs of a cross section of collecting compartment after one, three and five passes through the revolving static mixer are given in Fig. 4. It is obvious that the mixing quality strongly depends on the number of rotations. There is considerably high segregation of particles after only one pass through a mixer device.

Figure 4 presents the results of the experiment for three segmented Komax static mixer. To compare the results of the numerical simulation with experimental results, it was necessary to approximate results of experiment. The original computer code was developed for this purpose, [8].

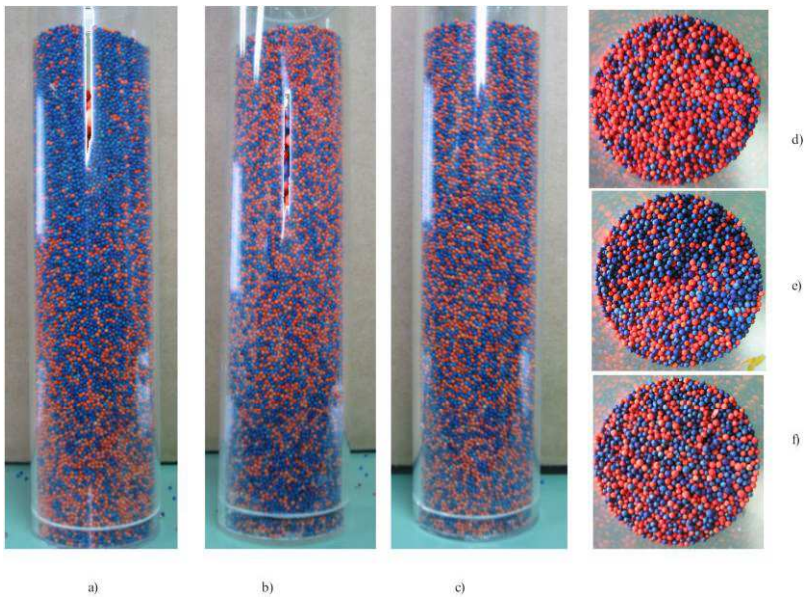

Figure 4. The results of the experiment after rotation of static mixer, with a) one material pass, b) three passes and c) five passes; cross-sections of the bottom compartment after d) one material pass, e) three passes and f) five passes.

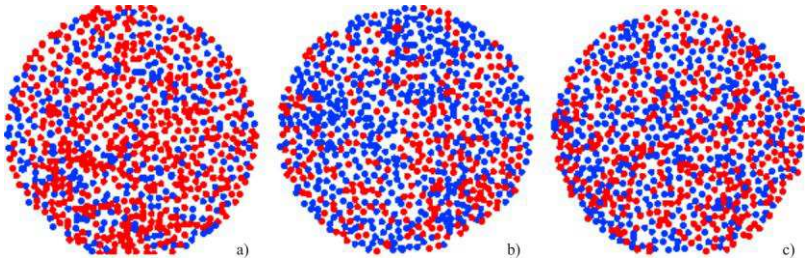

Figure 5. The results of the experiment after rotation of static mixer, with a) one material pass, b) three passes and c) five passes; cross-sections of the bottom compartment after d) one material pass, e) three passes and f) five passes.

Color images of experimental results were captured by a Sony PowerShot A550, which is a common digital camera for home use. All the acquired images were 24 bit RGB (16.8 millions of colors) with a 1024 x 768 spatial resolution. The macro function of the digital camera has been used, to cover a scene area of approximately Ø60 mm. Samples were placed on a white paper napkin set on a flat white painted surface, inside the closed chamber, 15cm below the digital camera. Paper napkins were used in order to avoid undesired reflection effects from chamber's walls. With this setup, it was possible to capture images with negligible shadows and without specular reflections.

For the elaboration of the images, every image file is imported into the originally developed computer program, [8]. Each image color data were transformed to the three-dimensional array of the R (red), G (green) and B (blue) values, ranging from 0-255.These data were processed in order to find the color of observed pixel and to change its R, G and B values to the closest color (red or blue). Fig. 5 presents the results of these calculations.

Figure 5. shows the transformed pictures taken from the camera, taken from the upside, when the material fell to the bottom compartment (shown on Fig. 4), prepared to be used for the mixing quality test. The obtained picture was divided into four quadrants (quarters) and the number of red and blue pixels was calculated for each quarter, and the homogeneity of the mixture is calculated on the basis of the relative standard deviation (RSD) criteria. The result of the numerical simulation was also tested upon the same conditions under which the experiments were conducted.

It will be shown that the numerical results are in good agreement with experimental results by comparing the quality of the mixing process, regarding RSD criterion, [38].

There were four rotations of the premixer, and it is possible to change the number of rotations as many times as it is necessary to optimize the mixing process. DEM analysis is the most reliable and most convincing method to optimize the mixing process according to mixing quality. The results of the numerical simulations are shown on Fig. 6. Figure 6 shows the trajectory, velocity and acceleration in x, y and z direction of one particle during four rotations of the mixer and the positions of the particles in the bottom cross section after 1-5 material passes through the revolving static mixer. The position of the representative particle is dramatically changed with the mixer revolutions, with significant turnovers in particle velocity and acceleration, which greatly contributes to the possibility of increased mixing quality.

The velocity and the pressure field of the gas phase were obtained via CFD calculations, Fig. 7a and 7b. This figure shows that the geometry of the Komax elements has influence on the velocity of the working fluid and supports the mixing. The trajectories of the mixing particles can also be obtained from DEM analysis. Figure 7c shows the trajectory of 8,000 particles through one pass of the mixer. Particle trajectory has influence on the mixing quality. Optimal prolonging of the trajectory contributes better homogeneity of the mixture, [8].

Poincare plot is used to visualize how particles mix. The Poincare plot places a colored dot for each particle at the location at which the particle passes through a cut plane (known as a Poincare section). In Figure 8, the locations of the particles at 12 Poincare sections are shown, during the first (Fig. 8a) and second (Fig. 8b) passes of the material. The color parameter is a logical expression used to mark the initial color of particles at positions $x<0$ (red) and $x>0$ (blue). The first Poincare section, the one furthest to the left in Fig. 8a clearly indicates which particles start with coordinates of $x < 0$. As the particles begin to fall, they begin to mix together. By the end of the mixer, the particles have not mixed completely - there are still significant pockets of only red and only blue particles.

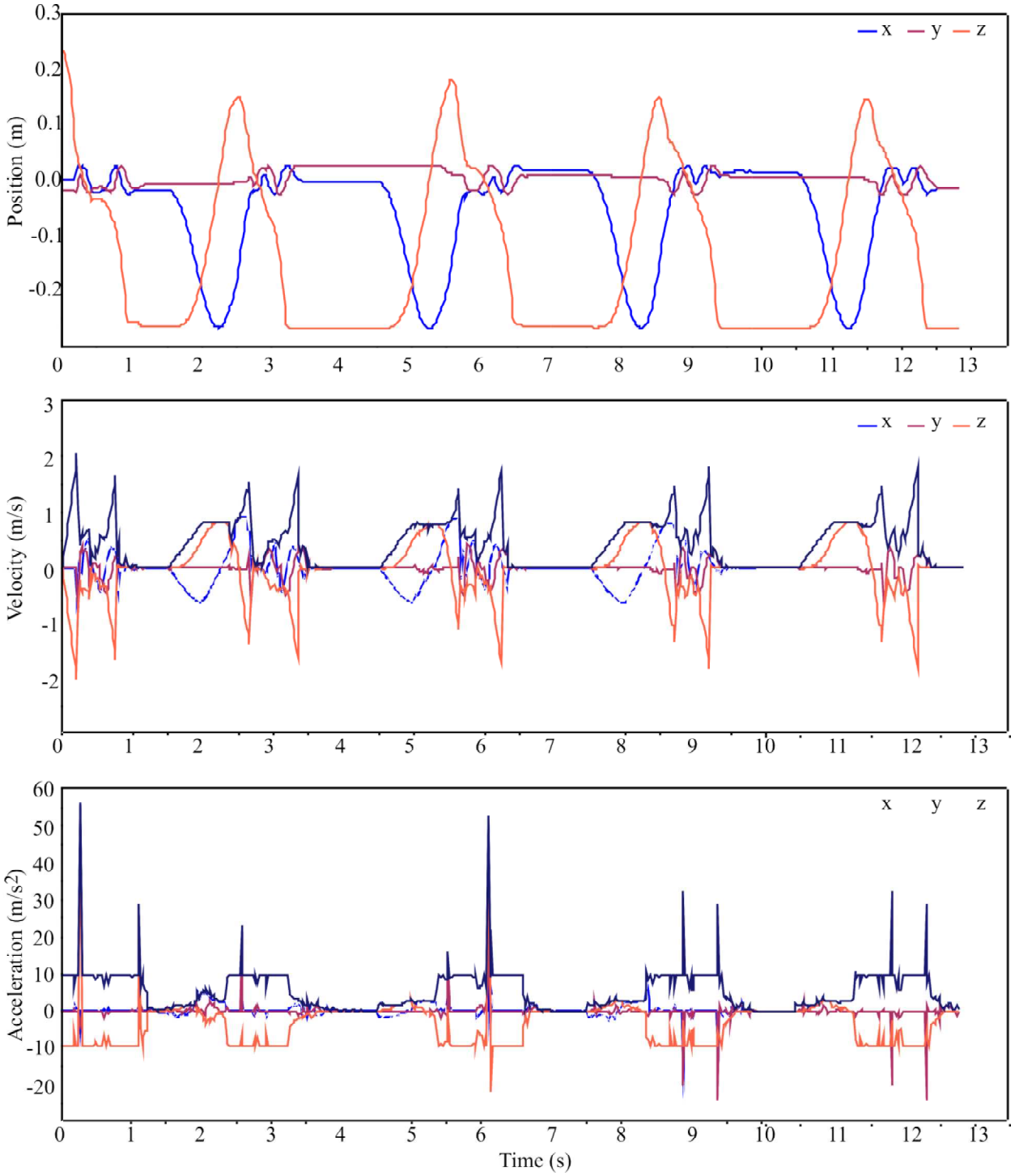

Figure 6. a) Trajectory, b) velocity and c) acceleration (in x, y and z direction) of one particle during the four rotations of static mixer.

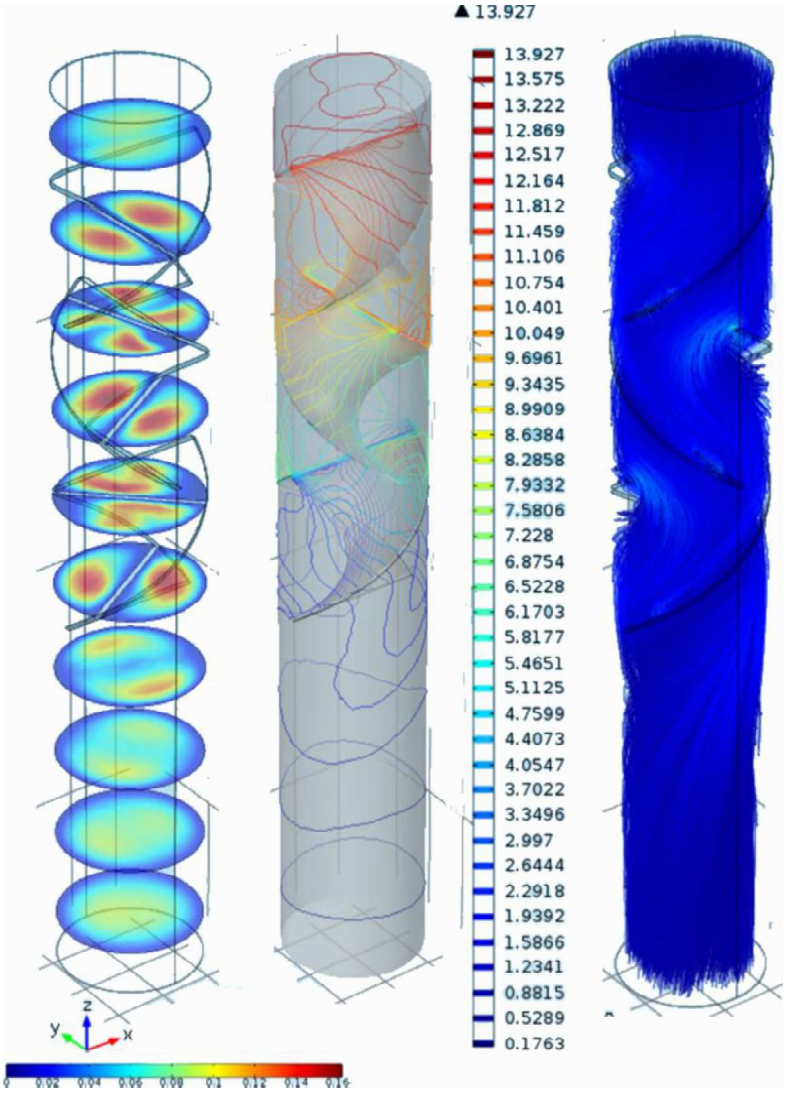

Figure 7. a) The magnitude value of the velocity, when the mixer is fully turned, b) the pressure field of the gas phase after first passing through the mixer, when the mixer is fully turned, c) the results of the numerical simulation (particle trajectories).

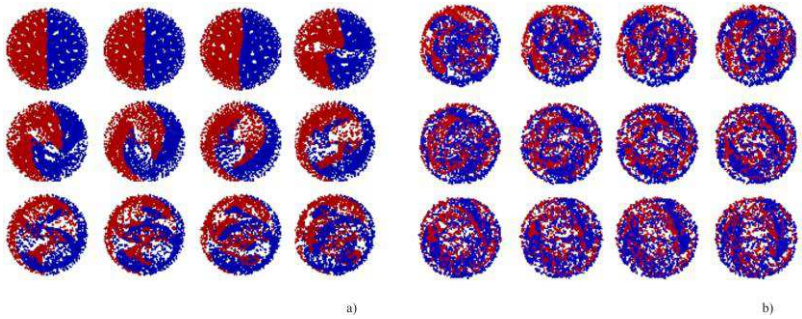

Figure 8. Poincare maps of the particle trajectories at different Poincare sections, during the a) first and 8b) second pass of the material.

The degree of mixing and the time needed to achieve an acceptable mixture can be predicted using here presented coupled DEM/CFD algorithms and experimental measurements. The literature has proposed several tools and indices to evaluate the degree of homogeneity of a mixture, [16,38,39]. In this work, the relative standard deviation (RSD) criterion was used to follow the evolution of mixing uniformity for the static mixers. RSD, which is a well-known mixing criterion in the pharmaceutical industry, is defined as:

$$RSD = \frac{\sigma}{\bar{x}} \cdot 100\%, \quad \sigma = \sqrt{\frac{\sum_{i=1}^{M} \bar{x} - x_i^{\,2}}{M-1}} \tag{13}$$

where M is the number of samples, x_i the concentration of a sample i and $\bar{x}$ the average concentration of all samples.

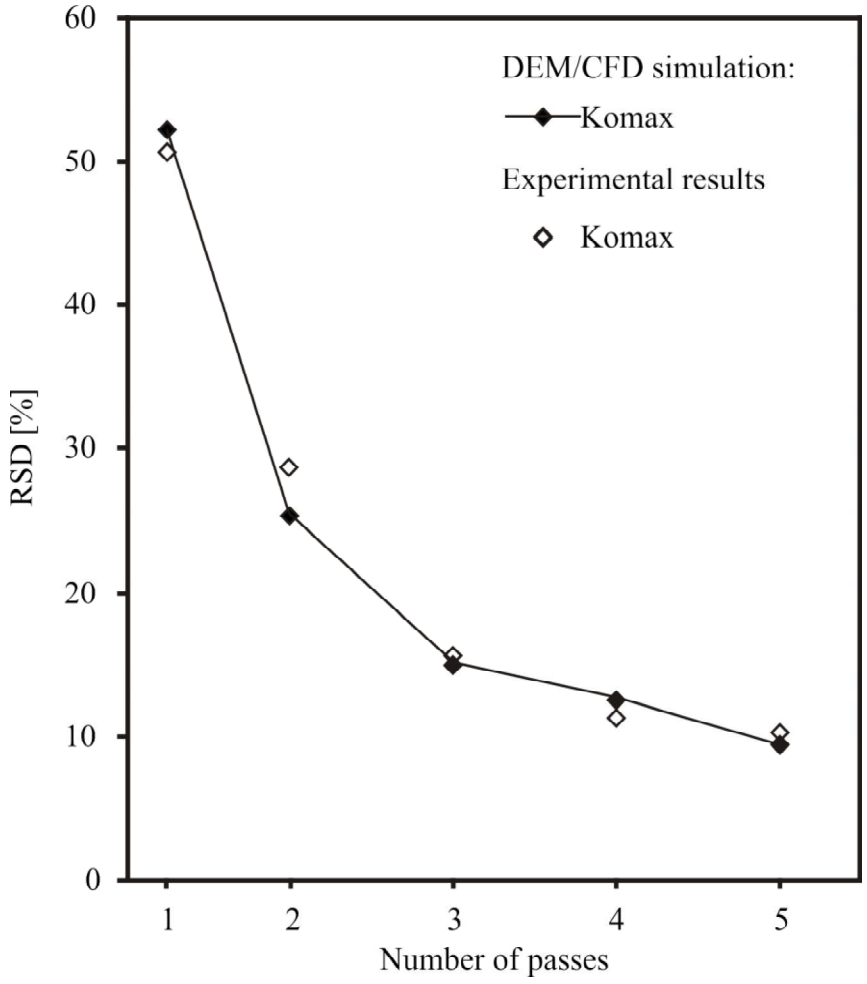

Figure 9. The relation between the RSD mixing criterion and the number of passes through the mixer.

The results of numerical simulations and experimental mixing processes are presented in Fig. 9. Mixing begins after particles leave the upper segment, between section 1 and 2, Fig. 9 (as soon as

the mobile panel is removed, enabling the granules to fall toward the revolving static mixer). The particles are rapidly blended in the first section, as seen from the figure, reaching the mixing degree of 50-52% at the outlet. After the second pass, the mixing quality reaches 25%, and after the third pass 16-17%. Additional rotations less contribute increasing the mixing quality and mixing degree reaches 12-13% and 10-11% after fourth and fifth material passes, respectively.

Figure 9 presents the relation between the RSD mixing criterion and the number of material passes through the mixer for numerical and experimental results. The RSD is decreasing significantly after first and second material passes, while the further decrease of RSD criteria is much slower for higher number of passes. From Fig. 9, it is obvious that 1) the RSD value is larger than 10%, 2) the homogeneity cannot be satisfactory after five passes through a revolving static mixer, and 3) the additional mixer should be used for the main mixing process. However, mixing time and energy consumption will be significantly reduced in the main mixing process (5-10 times, according to authors experiments and calculations).

CONCLUSION

Coupled DEM/CFD approach was used to investigate mechanisms of fluid flow and particle tracking for granular flow in revolving Komax static mixer. In the DEM, particle–particle and the particle–wall interactions are resolved and the time integration is carried out using Newton's laws of motion. CFD analysis was used to obtain velocity and pressure field for gas phase by using a mixture model. The particle trajectories with particle positions were tracked and analyzed in order to estimate the quality of the mixing process. The relative standard deviation mixing criterion is used for this purpose. Optimization of the number of rotations of the mixer was done by using mathematical modeling. The aim of this study was to predict the behavior of granules in revolving Komax static premixer. According to the results, this type of device can be used only as premixing device and additional mixer is necessary to gain the good quality of the mixture. The premixing process can contribute better quality of the mixure and can significantly reduce the mixing time and the cost of the mixing process.

Acknowledgments
This work was supported by the Ministry of Education, Science and Technological Development of the Republic of Serbia grant TR31055.

Reference

1. R. K Thakur, Ch.Vial, K. D. P. Nigam, E. B. Nauman, G. Djelveh, Static Mixers in the Process Industries – A Review, Trans IChemE, Vol 81, Part A, (2003) 787-826.
2. H. E. H. Meijer, M. K. Singh, P. D. Anderson, On the performance of static mixers: A quantitative comparison, Progress in Polymer Science, 37 (2012) 1333– 1349.
3. W.S. Sutherland, Improvement in apparatus for preparing gaseous fuel, UK Patent 1784 (1874).
4. M.J. Bakker, Dispositif pour preparer du beton ou une matiere analogue, French Patent 959,155(1949).
5. R.F. Stearns, Method and apparatus for continuous flow mixing, US Patent 2,645,463, assigned to Standard Oil Development Company (1953).

6. T.M. Beasey, Plate type fluid mixer, US Patent 3,382,534,assigned to Monsanto Company (1968).
7. J.E. Tollar, Interfacial surface generator, US Patent 3,239,197, assigned to The Dow Chemical Company (1966).
8. A. Jovanović, M. Pezo, L. Pezo, Lj. Lević, DEM/CFD Analysis of Granular Flow in Static Mixers, Powder Technology, 266 (2014) 240-248.
9. A. Ghanem, T. Lemenand, D. Della Valle, H. Peerhossaini, Static mixers: Mechanisms, applications and characterization methods – A review, Chemical Engineering Research and Design, 92 (2014) 205–228.
10. J. Bridgwater, Mixing of powders and granular materials by mechanical means-A perspective, Particuology, 10 (2012) 397– 427.
11. P. A. Cundall, O. D. L. Strack, A discrete numerical model for granular assemblies. Géotechnique, 29 (1979) 47–65.
12. H.P. Zhu, Z.Y. Zhou, R.Y. Yang, A.B. Yu, Discrete particle simulation of particulate systems: Theoretical developments, Chemical Engineering Science, 62 (2007) 3378 – 3396.
13. M. Alian, F. Ein-Mozaffari, S. R. Upreti, Analysis of the mixing of solid particles in a plowshare mixer via discrete element method (DEM), Powder Technology, 274 (2015) 77–87.
14. D. J. Parker, C. J. Broadbent, P. Fowles, M. R. Hawkesworth and P. McNeil, Positron emission particle tracking — a technique for studying _ow within engineering equipment, Nuclear Instrum. Methods Phys. Res. A326 (1993) 592–607.
15. B.F.C. Laurent, P.W. Cleary, Comparative study by PEPT and DEM for flow and mixing in a ploughshare mixer, Powder Technol. 228 (2012) 171–186.
16. P. Lacey, Developments in theory of particulate mixing, J.Appl. Chem., 4 (1954) 257–259.
17. D. Barrasso, T. Eppinger, F. E. Pereira, R. Aglave, K. Debus, S. K.Bermingham, R. Ramachandran, A multi- scale, mechanistic model of a wet granulation process using a novel bi-directional PBM–DEM coupling algorithm, Chemical Engineering Science, 123 (2015) 500–513.
18. G.R. Chandratilleke, A.B.Yu, J.Bridgwater, A DEM study of the mixing of particles induced by a flat blade, Chemical Engineering Science, 79 (2012) 54–74.
19. K.W. Chu, B.Wang, D.L.Xu, Y.X.Chen, A.B.Yu, CFD–DEM simulation of the gas–solid flow in a cyclone separator, Chemical Engineering Science, 66 (2011) 834–847.
20. J. Neuwirth, S. Antonyuk, S. Heinrich, M. Jacob, CFD–DEM study and direct measurement of the granular flow in a rotor granulator, Chemical Engineering Science, 86 (2013) 151–163.
21. D. Liu, C. Bu, X. Chen, Development and test of CFD-DEM model for complex geometry: A coupling algorithm for Fluent and DEM, Computers and Chemical Engineering, 58 (2013) 260-268.
22. M. Halidan, G.R.Chandratilleke, S.L.I.Chan, A.B.Yu, J.Bridgwater, Prediction of the mixing behaviour of binary mixtures of particles in a bladed mixer, Chemical Engineering Science, 120 (2014) 37–48.
23. B. Remy, J. G. Khinast, B. J. Glasser, Polydisperse granular flows in a bladed mixer: Experiments and simulations of cohesionless spheres, Chemical Engineering Science, 66 (2011) 1811–1824.
24. M. Jiang, Y. Zhao, G. Liu, J. Zheng, Enhancing mixing of particles by baffles in a rotating drum mixer, Particuology, 9 (2011) 270–278.

25. S.J. Chen, L.T. Fan, C.A. Watson, The mixing of solids particles in a motionless mixer—a stochastic approach, AIChE Journal, 18 (5) (1972) 984–989.
26. R.H. Wang, L.T. Fan, Axial mixing of grains in a motionless Sulzer (Koch) mixer, Industrial & Engineering Chemistry: Process Design & Development, 15 (3) (1976) 381–388.
27. R.H. Wang, L.T. Fan, Stochastic modelling of segregation in a motionless mixer, Chemical Engineering Science, 32 (1977) 695–701.
28. D. Ponomarev, V. Mizonov, H. Berthiaux, C. Gatumel, J. Gyenis, E. Barantseva, A 2D Markov chain for modelling powder mixing in alternately revolving static mixers of Sysmix® type, Chemical Engineering and Processing, 48 (2009) 1495–1505.
29. D. Ponomarev, V. Mizonov, C. Gatumel, H. Berthiaux, E. Barantseva, Markov-chain modelling and experimental investigation of powder-mixing kinetics in static revolving mixers, Chemical Engineering and Processing, 48 (2009) 828–836.
30. R.O. Fox, L.T. Fan, Stochastic analysis of axial solids mixing in a fluidized bed, in: 1st World Congress on Particle Technology, vol. III, Nuremberg (1986) 581.
31. H.G. Dehling, A.C. Hoffman, H.W. Stuut, Stochastic models for transport in a fluidised bed, SIAM Journal of Applied Mathematics, 60 (1) (1999) 337–358.
32. L.T. Fan, S.H. Shin, Stochastic diffusion model of non-ideal mixing in a horizontal drum mixer, Chemical Engineering Science, 34 (1979) 811–820.
33. M. Aoun Habbache, M. Aoun, H. Berthiaux, V. Mizonov, An experimental method and a Markov chain model to describe axial and radial mixing in a hoop mixer, Powder Technology, 128 (2002) 159– 167.
34. D.M. Hobbs, F.J. Muzzio, Reynolds number effects on laminar mixing in the Kenics static mixer. Chem. Eng. J. , 70 (2) (1998) 93–104.
35. D.M. Hobbs, P.D. Swanson, F.J. Muzzio, Numerical characterization of low Reynolds number flow in the Kenics static mixer. Chem. Eng. Sci., 53 (8) (1998) 1565–1584.
36. V. Kumar, V. Shirke, K.D.P. Nigam, Performance of Kenics static mixer over a wide range of Reynolds number. Chem.Eng. J., 139 (2) (2008) 284–295.
37. J. J. McCarthy, D. V. Khakhar, J. M. Ottino, Computational studies of granular mixing, Powder Technology, 109 (2000) 72–82.
38. A. Lemieux, G. Leonard, J. Doucet, L. A. Leclaire, F. Viens, J. Chaouki, Large-scale numerical investigation of solids mixing in a V-blender using the discrete element method, Powder Technology, 181 (2008) 205–216.
39. M. Poux, P. Fayolle, J. Bertrand, Powder mixing: some practical rules applied to agitated systems, Powder Technology, 68 (1991) 213-234.
40. J. Lin, X. F. Shu, J. X. Dong, The experimental determination of mechanical properties of zeolite ferrierite crystal, Materials Letters, 59 (12) (2005) 1595–1597.
41. H.P. Zhu, Z.Y. Zhou, R.Y. Yang, A.B. Yu, Discrete particle simulation of particulate systems: A review of major applications and findings, Chemical Engineering Science, 63 (2008) 5728 – 5770.
42. S. V. Patankar, Numerical Heat Transfer and Fluid Flow, Hemisphere Publishing Corporation, 1980.
43. C. E. Smith, P. Liu, Coefficient of restitution. Journal of Applied Mechanics 59 (4) (1992) 963-969.
44. R.Y. Yang, Zou R.P., Yu A.B., Microdynamic analysis of particle flow in a horizontal rotating drum, Powder Technology, 130 (2003) 138-146.
45. G. J. LoCurto, X. Zhang, V. Zarikov, R. A. Bucklin, L. Vu-Quoc, D. M. Hanes, O. R.

Walton. Soybean impacts: experiments and dynamic simulations. Transactions of the ASAE 40 (3) (1997) 789-794.
46. N. N. Mohsenin. Physical Properties of Plant and Animal Materials. 2nd ed. New York: Gordon and Breach Science Publishers, 1986.
47. Stahl, B. M. Grain bin requirements. USDA Circular 835. Washington, D.C.: U.S. Department of Agriculture, 1950.
48. M. J. Jiang, H. S. Yu, and D. Harris. A novel discrete model for granular material incorporating rolling resistance. Computers and Geotechnics 32 (5) (2005) 340-357.

Figure captions

Figure 1. Schematic design of the revolving static mixer industrial application, (1) silos, (2) screw conveyor, (3) weighting scale, (4) revolving static mixer, (5) main mixer.

Figure 2. a) Scheme of the revolving static mixer, b) Experimental configuration, c) Komax mixer.

Figure 3. Rotation of the revolving static mixer.

Figure 4. The results of the experiment after rotation of static mixer, with a) one material pass, b) three passes and c) five passes; cross-sections of the bottom compartment after d) one material pass, e) three passes and f) five passes.

Figure 5. The results of the approximation of the experimental results after a) one material pass, b) three passes and c) five passes

Figure 6. a) Trajectory, b) velocity and c) acceleration (in x, y and z direction) of one particle during the four rotations of static mixer.

Figure 7. a) The magnitude value of the velocity, when the mixer is fully turned, b) the pressure field of the gas phase after first passing through the mixer, when the mixer is fully turned, c) the results of the numerical simulation (particle trajectories).

Figure 8. Poincare maps of the particle trajectories at different Poincare sections, during the a) first and 8b) second pass of the material.

Figure 9. The relation between the RSD mixing criterion and the number of passes through the mixer.

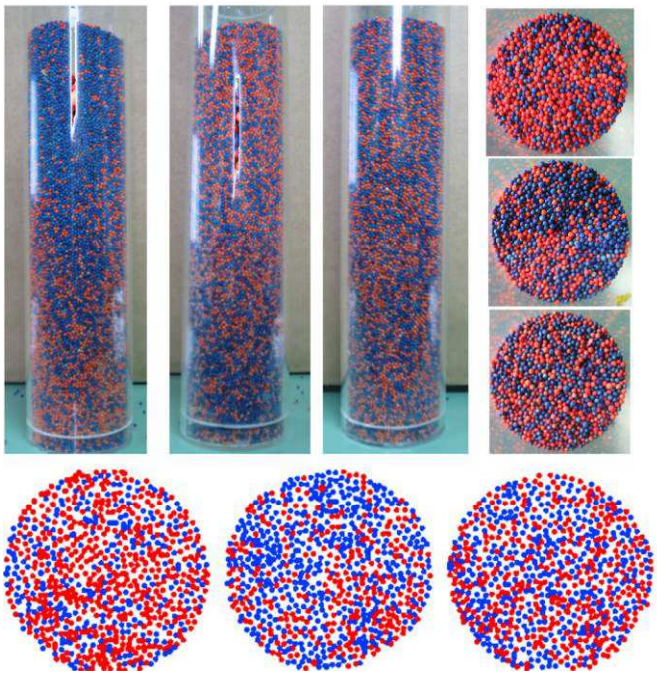

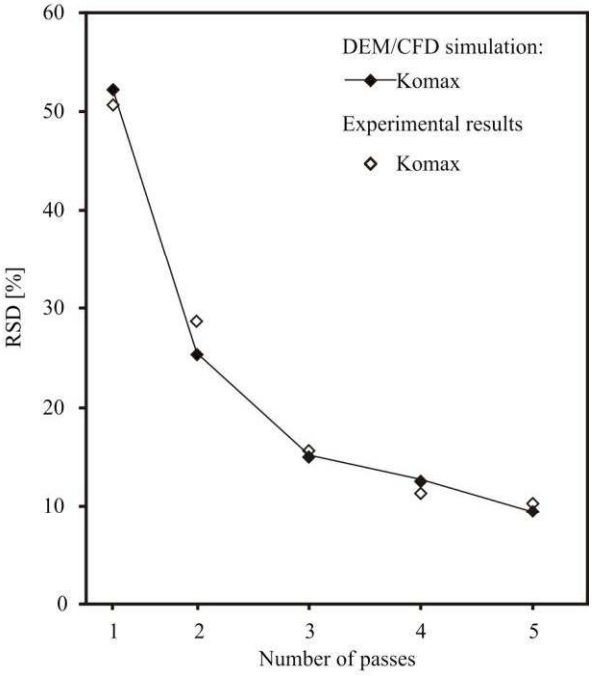

Highlights

- We did experiments for Komax revolving static mixer.
- Coupling DEM/CFD method was used for modeling granular flow in mixer.
- We predicted the behavior of particles in mixer after several rotations.
- We did optimization of mixers geometry based on mixing quality.